ISSN: 3033-3652

Journal of Physical Mathematics & its Applications

SCIENTIFIC Research and Community

Review Article

Open Access

Regularized Urysohn Operators for Nonlinear Systems with Memory: Theory, Numerical Methods, and Applications to Artificial Intelligence and Combustion

Manuel J Alves[1]* and Elena V Alves[2]

[1]Independent Researcher, Maputo, Mozambique-ORCID: 0000-0003-3713-155X

[2]Department of Quantitative Methods, ISCTEM, Maputo, Mozambique- ORCID: 0009-0000-1452-2553

ABSTRACT

Nonlinear systems with memory arise in learning algorithms, hereditary mechanics, biological regulation, combustion, and other processes whose present state depends on a distributed history of the unknown. This paper develops a compact mathematical and computational framework for regularized Urysohn operators acting on Banach spaces of continuous trajectories. We consider nonlinear integralmemory models of the form $u(t) = g(t) + \int_0^T K(t,s,u(s),u(t-\tau(s)))\,ds,$ and their regularized counterparts $u_\varepsilon(t) + \varepsilon L u_\varepsilon(t) = g(t) + \int_0^T K(t,s,u_\varepsilon(s),u_\varepsilon(t-\tau(s)))\,ds, \quad \varepsilon > 0,$ where L is a stabilizing positive operator and K is a nonlinear Urysohn kernel. Under natural continuity, growth, Lipschitz, and compactness assumptions we prove existence, uniqueness, a priori estimates, compactness of approximate solutions, stability with respect to data, and convergence as the regularization parameter tends to zero. We also present Nyström and collocation schemes, derive practical error estimates, and give algorithms for Picard and damped Newton iterations. Two application modules are discussed: memory-augmented artificial intelligence models, where Urysohn terms represent nonlinear temporal attention or reservoir-type memory, and solid-propellant combustion, where the kernel captures thermal memory and pressure-dependent burning laws. The numerical illustrations emphasize regularization convergence, stability regions, parameter sensitivity, and comparison of discretization methods. The results show that regularized Urysohn operators provide a flexible bridge between rigorous nonlinear analysis and computational models with memory.

***Corresponding author**

Manuel J Alves, Independent Researcher, Maputo, Mozambique. ORCID: 0000-0003-3713-155X.

Received: January 27, 2026; **Accepted:** August 10, 2026; **Published:** August 24, 2026

Keywords: Urysohn Operator, Nonlinear Integral Equation, Regularization, Memory Effects, Compactness, Stability, Nyström Method, Artificial Intelligence, Combustion Modelling, Thermal Memory

MSC 2020: 45G10; 47H30; 47A52; 65R20; 68T07; 80A25.

Introduction

Many nonlinear phenomena cannot be described adequately by instantaneous laws. In learning systems, the response of a network depends on past inputs and internal states; in combustion, the local burning rate is affected by a history of heat release and pressure variations; in materials and biological regulation, hereditary terms determine the observed dynamics. Integral operators of Urysohn type form a natural language for such systems because they combine nonlinearity, nonlocality, and memory in a single mathematical object [1-3] Let $I = [0, T]$ and let $u : I \to \mathbb{R}^m$ be an unknown trajectory. A typical Urysohn operator has the form

$$(\mathcal{U}u)(t) = \int_0^T K(t,s,u(s))\,ds, \qquad (1)$$

where K is nonlinear in the state variable. In memory models the kernel may also depend on delayed values, distributed histories, or filtered states. Compared with Hammerstein or Volterra operators, the Urysohn formulation is sufficiently general to cover nonlinear kernels that change with both observation time and memory time [4-6]. This makes it suitable for systems where the past is not merely additive but transforms the current dynamics through a nonlinear law. The analytical difficulty is that Urysohn equations may be ill-conditioned. Small perturbations in the data or in the kernel may produce large changes in the solution, especially when the inverse problem is involved, when observations are noisy, or when the memory operator is nearly singular. This sensitivity is amplified by nonlinear feedback, because an error introduced at one point of the history can be propagated through the integral kernel and returned to the system at later times. Moreover, the state-dependent character of the kernel prevents the direct use of many linear Fredholm or Volterra techniques: compactness must be combined with nonlinear growth control, and stability must be obtained without destroying the memory structure. Regularization is therefore essential [7,8]. In this paper we introduce a stabilizing term εLu, where $\varepsilon > 0$ and L is a positive operator. The regularized problem is better conditioned, admits stable numerical schemes, and converges to a solution of the original problem under compactness and consistency assumptions. The parameter ε is interpreted not only as a numerical device but also as a modelling scale that penalizes unrealistic rough memory profiles, suppresses spurious high-frequency oscillations, and separates physically meaningful hereditary effects from numerical artifacts generated by discretization or noisy observations. The aim is threefold. First, we present a concise theory for regularized Urysohn operators in spaces of continuous trajectories, emphasizing assumptions that are easy to verify in applied kernels. Second, we describe implementable numerical methods and error indicators, with particular attention to the balance between discretization error and regularization error. Third, we connect the abstract theory to two application domains: artificial intelligence with memory and nonlinear combustion with thermal delay. These examples were chosen because both contain feedback, nonlocal dependence, and stability constraints, yet they arise in very different scientific communities. The same operator framework therefore provides a common language for rigorous analysis, algorithm design, and interpretation of nonlinear memory effects.

Novel Contributions

This paper is intended as a unified contribution rather than as a collection of disconnected examples. Relative to the classical literature on nonlinear integral equations, and also relative to recent work on neural operators, neural integral equations, and combustion modelling, the novelty is concentrated in the following points.

- We develop a unified theoretical framework for regularized Urysohn operators with statedependent memory, delayed arguments, and distributed-history effects in spaces of continuous trajectories.
- We establish stability, compactness, convergence, and robustness results for the regularized equation, including explicit error bounds with respect to the regularization parameter, perturbations of the data, and perturbations of the memory kernel.
- We connect the abstract analysis with two modern application domains that are usually treated separately: memory-augmented artificial intelligence and AP/HTPB solid-propellant combustion with thermal memory.
- We formulate Nyström, collocation, and Galerkin methods within the same operator-theoretic setting and explain how regularization controls both analytic ill-posedness and numerical conditioning.
- We add a spectral viewpoint based on resolvent operators, spectral radius estimates, and eigenvalue localization, providing a bridge between fixed-point stability and computational stability maps.

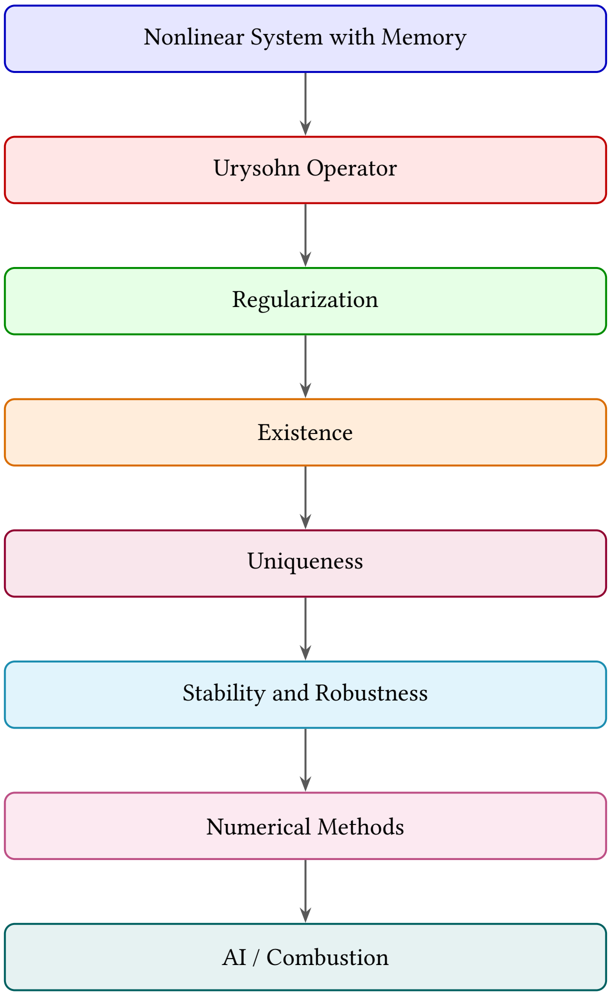

Figure 1: General Workflow of the Regularized Urysohn Methodology

Preliminaries and Urysohn Operators

Let $\mathcal{X} = C(I;\mathbb{R}^m)$ with norm $\|u\|_\infty = \max_{t\in I} |u(t)|$.

For $r > 0$ define $B_r = \{u \in \mathcal{X} : \|u\|_\infty \le r\}$. Let $\theta : I \times I \to I$ be a measurable memory map; in applications $\theta(t,s) = s,\ \theta(t,s) = t - s,$ or $\theta(t,s) = t - \tau(s)$

with boundary extension for negative arguments. We write

$$(\mathcal{K}u)(t) = \int_0^T K(t,s,u(s),u(\theta(t,s)))\,ds, \qquad (2)$$

where $K : I \times I \times \mathbb{R}^m \times \mathbb{R}^m \to \mathbb{R}^m$.

Definition 2.1: The operator $\mathcal{K} : \mathcal{X} \to \mathcal{X}$ defined by (2) is called a nonlinear Urysohn memory operator if K is measurable in s, continuous in (t, x, y) for almost every s, and maps bounded subsets of $\mathcal{X}$ into equicontinuous bounded subsets of $\mathcal{X}$.

We impose the following assumptions.
(A1) g $\in \mathcal{X}$ and K is a Carathéodory kernel.
(A2) For each $r > 0$ there exists $a_r \in L^1(0,T)$ such that $|K(t,s,x,y)| \le a_r(s)$ whenever $|x|$, $|y| \le r$.
(A3) For each $r > 0$ there exists $\ell_r \in L^1(0,T)$ such that

$$|K(t,s,x_1,y_1) - K(t,s,x_2,y_2)| \le \ell_r(s)(|x_1 - x_2| + |y_1 - y_2|)$$

for bounded arguments.

(A4) For bounded arguments, $K(t, s, x, y)$ is uniformly continuous in t for almost every s, with an integrable modulus.

Assumptions (A1)–(A4) ensure that K is continuous and compact on bounded subsets of X. These continuity assumptions are consistent with recent work on Urysohn operators in spaces of continuous and essentially bounded vector functions [9-11]. The compactness follows from the Arzelà-Ascoli theorem [12-13].

Lemma 2.2 (Compactness). Under *(A1)*–*(A4)*, the Urysohn memory operator $\mathcal{K}$ maps bounded subsets of $\mathcal{X}$ into relatively compact subsets of $\mathcal{X}$.

Proof. Let $u \in B_r$. By (A2), $\|\mathcal{K}u\|_\infty \le \int_0^T a_r(s)\,ds$. For $t_1, t_2 \in I$, (A4) gives

$$|(\mathcal{K}u)(t_1) - (\mathcal{K}u)(t_2)| \le \int_0^T \omega_r(|t_1 - t_2|, s)\,ds,$$

where the right-hand side tends to zero as $t_1 \to t_2$ by dominated convergence. Thus $\mathcal{K}(B_r)$is bounded and equicontinuous. Arzelà-Ascoli yields relative compactness.

Regularized Nonlinear Memory Model

Building on classical regularization and nonlinear integral-equation theory we study the unregularized equation [2,6-8]

$$u = g + \mathcal{K}u \qquad (3)$$

and the regularized equation

$$u_\varepsilon + \varepsilon L u_\varepsilon = g + \mathcal{K}u_\varepsilon, \quad \varepsilon > 0. \qquad (4)$$

Here $L : D(L) \subset \mathcal{X} \to \mathcal{X}$ is a linear stabilizing operator. In computations L may be a discrete derivative, a graph-Laplacian memory smoother, or simply the identity. For the abstract results we assume:

(R1) For every $\varepsilon > 0$, $R_\varepsilon = (I + \varepsilon L)^{-1}$ exists and is bounded on $\mathcal{X}$.

(R2) $\|R_\varepsilon\| \le 1$ and $R_\varepsilon v \to v$ in $\mathcal{X}$ for every $v \in \mathcal{X}$ as $\varepsilon \downarrow 0$.

Then (4) is equivalent to

$$u_\varepsilon = R_\varepsilon(g + \mathcal{K}u_\varepsilon). \qquad (5)$$

Regularization therefore changes the fixed-point operator from $g+K$ to $R\varepsilon(g+K)$, preserving compactness while improving stability. This transformation is important because it does not remove the nonlinear memory mechanism; it only filters the component of the response that is incompatible with the stabilizing scale imposed by L. In practical computations, this means that the hereditary part of the model remains visible, while oscillatory modes caused by insufficient data resolution, noisy kernels, or excessive feedback are attenuated before they contaminate the fixed-point iteration.

Scope of the Regularization Assumptions

Assumptions (R1)–(R2) are deliberately stated at the resolvent level. They do not assert that regularization automatically makes every nonlinear problem well posed. Existence still requires the invariant-ball condition, uniqueness and Lipschitz stability are obtained in the contraction regime, and convergence to the unregularized model additionally requires a uniform a priori bound. The phrase "improved conditioning" is therefore used in the numerical sense: for the discrete systems considered below, the stabilizing term shifts or damps poorly resolved modes and can reduce sensitivity of the nonlinear solve. The amount of improvement depends on the choice of L, ε, the discretization, and the spectrum of the linearized operator; it is not claimed to be uniform for all admissible kernels. Importantly, the nonlinear Urysohn term Ku is retained unchanged, so the state-dependent memory structure is preserved rather than replaced by a linear surrogate.

Main Theoretical Results

Existence

Theorem 4.1: (Existence of a regularized solution). Assume *(A1)*–*(A4)* and *(R1)*–*(R2)*. Suppose there exists $r > 0$ such that

$$\|g\|_\infty + \int_0^T a_r(s)\,ds \le r. \qquad (6)$$

Then for every $\varepsilon > 0$ *equation* (4) *has at least one solution* $u_\varepsilon \in B_r$.

Proof. Define $\Phi_\varepsilon(u) = R_\varepsilon(g + \mathcal{K}u)$. If $u \in B_r$, then by (6) and $\|R_\varepsilon\| \le 1$, $\|\Phi_\varepsilon(u)\|_\infty \le r$. The operator $\Phi\varepsilon$ is continuous and compact because $R\varepsilon$ is bounded and K is compact on bounded sets. Schauder's fixed point theorem gives a fixed point $u_\varepsilon \in B_r$ [2-13].

Uniqueness and Contraction Regime

Let $L_r = \int_0^T \ell_r(s)\,ds$.

Theorem 4.2: (Uniqueness). *Assume the hypotheses of the existence theorem. If* $2L_r < 1$, *then the regularized problem (4) has a unique solution in* B_r.

Proof. For $u, v \in B_r$,

$$\|\Phi_\varepsilon(u) - \Phi_\varepsilon(v)\|_\infty \le \|\mathcal{K}u - \mathcal{K}v\|_\infty \le 2L_r\,\|u - v\|_\infty.$$

Thus $\Phi\varepsilon$ is a contraction on B_r. Banach's fixed-point theorem gives uniqueness [13,14].

A Priori Estimates and Stability

Proposition 4.3: (A priori estimate). If $u\varepsilon$ solves (4) in B_r, then

Proof. The first estimate follows directly from (5). The second follows by inserting the linear growth bound and collecting the term $\|u_\varepsilon\|_\infty$ on the left-hand side.

Theorem 4.4: (Stability with respect to data). *Let* u_ε and $\tilde{u}_\varepsilon$ solve regularized equations with data (g,K) and $(\tilde{g},\tilde{K})$ in B_r. Assume $2L_r < 1$ and

$$\Delta_K = \sup_{t\in I,\ u\in B_r} \left|(\mathcal{K}u)(t) - (\tilde{\mathcal{K}}u)(t)\right|. \tag{7}$$

If *K has linear growth* $|K(t,s,x,y)| \le c_0(s) + c_1(s)(|x|+|y|)$, *then*

$$\|u_\varepsilon\|_\infty \le \frac{\|g\|_\infty + \|c_0\|_{L^1}}{1 - 2\|c_1\|_{L^1}}, \quad 2\|c_1\|_{L^1} < 1. \tag{8}$$

Proof. The first estimate follows directly from (5). The second follows by inserting the linear growth bound and collecting the term $\|u_\varepsilon\|_\infty$ on the left-hand side.

Theorem 4.4 (Stability with respect to data). *Let* u_ε and $\tilde{u}_\varepsilon$ solve regularized equations with data (g,K) and $(\tilde{g},\tilde{K})$ in B_r. *Assume* $2L_r < 1$ and

$$\Delta_K = \sup_{t\in I,\ u\in B_r} \left|(\mathcal{K}u)(t) - (\tilde{\mathcal{K}}u)(t)\right|.$$

Then

$$\|u_\varepsilon - \tilde{u}_\varepsilon\|_\infty \le \frac{\|g-\tilde{g}\|_\infty + \Delta_K}{1 - 2L_r}. \tag{9}$$

Proof. Subtract the two fixed point equations and use the Lipschitz estimate:

$$\|u_\varepsilon - \tilde{u}_\varepsilon\|_\infty \le \|g-\tilde{g}\|_\infty + \Delta_K + 2L_r\|u_\varepsilon - \tilde{u}_\varepsilon\|_\infty.$$

The result follows by rearrangement.

Robustness under Noisy Memory Kernels

In applications the memory kernel is rarely known exactly. In AI it may be learned from data, and in combustion it may be inferred from pressure-temperature measurements. The next result shows that small errors in the kernel produce small errors in the regularized solution.

Theorem 4.5: (Robustness under noisy memory kernels). Let K and K^δ be two memory kernels satisfying the same Lipschitz condition on B_r, with $2L_r < 1$. Suppose

$$\sup_{t\in I,\,|x|,|y|\le r} \int_0^T |K(t,s,x,y) - K^\delta(t,s,x,y)|\,ds \le \delta.$$

Let u_ε and u_ε^δ be the corresponding regularized solutions with the same data g. Then

$$\|u_\varepsilon - u_\varepsilon^\delta\|_\infty \le \frac{\delta}{1-2L_r}. \tag{10}$$

Consequently, noisy thermal-memory kernels or learned neural kernels are stable in the solution norm whenever the feedback remains in the contraction regime.

Proof. Subtract the two fixed-point equations. The perturbation of the kernel contributes at most δ, while the difference of the two solutions is multiplied by the same Lipschitz factor $2L_r$. Hence

$$\|u_\varepsilon - u_\varepsilon^\delta\|_\infty \le \delta + 2L_r\|u_\varepsilon - u_\varepsilon^\delta\|_\infty.$$

Rearranging gives (10).

Compactness and Convergence of Regularization

Theorem 4.6: (Asymptotic compactness of regularized solutions). Assume (*A*1)–(*A*4), (*R*1)–(*R*2), and the uniform a priori bound $\|u_\varepsilon\|_\infty \le r$ *for* $0 < \varepsilon \le \varepsilon_0$. Then, for every sequence $\varepsilon_n \downarrow 0$, the sequence $\{u_{\varepsilon_n}\}$ is relatively compact in $\mathcal{X}$.

Proof. Set $v_n = g + \mathcal{K}u_{\varepsilon_n}$. Because $\{u_{\varepsilon_n}\} \subset B_r$ and $\mathcal{K}$ is compact on bounded sets, $\{v_n\}$ is relatively compact. After passage to a subsequence, $v_n \to v$ in $\mathcal{X}$. The uniform bound $\|R\varepsilon\| \le 1$ and the strong convergence $R\varepsilon v \to v$ imply

$$\|R_{\varepsilon_n}v_n - v\|_\infty \le \|R_{\varepsilon_n}(v_n - v)\|_\infty + \|R_{\varepsilon_n}v - v\|_\infty \to 0.$$

Since $u_{\varepsilon_n} = R_{\varepsilon_n}v_n$, the selected subsequence converges in $\mathcal{X}$ This proves the asymptotic compactness needed for the limit ε ↓ 0 without imposing an unproved collective-compactness property on the resolvent family.

Theorem 4.7: *(Convergence as ε ↓ 0). Let* u_ε *be solutions of (4) with a uniform bound in* B_r. *Then every sequence* $\varepsilon_n \downarrow 0$ *contains a subsequence such that* $u_{\varepsilon_n} \to u$ in, $\mathcal{X}$ *where u solves the unregularized equation (3). If (3) has a unique solution in* B_r, *then* $u_\varepsilon \to u$ *in* $\mathcal{X}$ *as ε ↓ 0.*

Proof. By compactness, take $u_{\varepsilon_n} \to u$ in $\mathcal{X}$. Since $\mathcal{K}$ is continuous, $\mathcal{K}u_{\varepsilon_n} \to \mathcal{K}u$. From $u_{\varepsilon_n} = R_{\varepsilon_n}(g + \mathcal{K}u_{\varepsilon_n})$ and $R_{\varepsilon_v} \to v$, we pass to the limit and obtain $u = g + \mathcal{K}u$. If the limit solution is unique, all subsequences have the same limit, hence the whole family converges.

Corollary 4.8: (Convergence rate in the contraction case). *Assume* $2L_r < 1$ *and suppose the exact solution u belongs to D(L) with* $\|Lu\|_\infty < \infty$. *If the same kernel is used in (3) and (4), then*

$$\|u_\varepsilon - u\|_\infty \le \frac{\varepsilon\|Lu\|_\infty}{1-2L_r}. \tag{11}$$

Proof. Use $u + \varepsilon L_u = g + \mathcal{K}u + \varepsilon L_u$ and subtract the regularized equation. The contraction estimate gives $(1 - 2L_r)\|u_\varepsilon - u\|_\infty \le \varepsilon\|Lu\|_\infty$.

Spectral Properties of Regularized Urysohn Operators

Although the Urysohn operator is nonlinear, spectral information can be obtained from its linearization around a solution. Let u_ε be a regularized solution and assume that $\mathcal{K}$ is Fréchet differentiable with respect to the state variables. Define the linearized memory operator

$$(A_\varepsilon v)(t) = \int_0^T \Big[K_x(t,s,u_\varepsilon(s),u_\varepsilon(\theta(t,s)))v(s) + K_y(t,s,u_\varepsilon(s),u_\varepsilon(\theta(t,s)))v(\theta(t,s))\Big]ds.$$

The linearized fixed-point map is $R_\varepsilon A_\varepsilon$. Its spectral radius controls local stability of the regularized solution.

Theorem 5.1: *(Spectral stability criterion). Assume A_ε is compact on $\mathcal{X}$ and R_ε is bounded. If*

$$r(R_\varepsilon A_\varepsilon) < 1,$$

then $I - R_\varepsilon A_\varepsilon$ is invertible and the regularized solution is locally stable under small perturbations of the data and the kernel. Moreover, the resolvent is represented by the Neumann series

$$(I - R_\varepsilon A_\varepsilon)^{-1} = \sum_{k=0}^{\infty} (R_\varepsilon A_\varepsilon)^k$$

whenever $\|R_\varepsilon A_\varepsilon\| < 1$.

Proof. If the spectral radius is smaller than one, the point 1 belongs to the resolvent set of $R_\varepsilon A_\varepsilon$.Therefore $I - R_\varepsilon A_\varepsilon$ is invertible. When the operator norm is smaller than one, the inverse is given by the usual Neumann series. The implicit-function argument for the linearized equation then gives local stability.

Proposition 5.2: (Eigenvalue localization). *If $\|A\varepsilon\| \le \kappa$ and $\|R_\varepsilon\| \le 1$, then every eigenvalue λ of $R_\varepsilon A_\varepsilon$ satisfies $|\lambda| \le \kappa$. In particular, the contraction condition $\kappa < 1$ implies spectral stability.*

Proof. The estimate follows from $r(R_\varepsilon A_\varepsilon) \le \|R_\varepsilon A_\varepsilon\| \le \|A_\varepsilon\| \le \kappa$.

The resolvent formulation is useful computationally because it relates Newton conditioning, stability maps, and bifurcation indicators to the same object [6,13]. Eigenvalues close to the unit circle signal loss of local stability, while the regularization operator shifts the spectrum toward a safer region by damping rough memory modes.

Comparison with Recent Literature (2023–2026)

Recent publications confirm that nonlinear integral equations, regularization, and operator learning are developing along convergent lines. Work on regularization of nonlinear Fredholm and Volterraintegral equations has emphasized convergence under noisy or ill-conditioned data, but usually without connecting the regularized equation to memory-based AI and combustion applications [15, 16].Recent numerical work on Urysohn-type equations has also strengthened collocation and approximation techniques, yet the spectral and robustness aspects are often separated from the numerical discussion [17-19]. In parallel, neural operators, Fourier neural operators, neural integral equations, and temporal neural operators have become central tools for learning maps between function spaces [20-22]. These models learn nonlocal transformations from data, while the present paper supplies a deterministic regularized Urysohn framework in which such nonlocal learning layers can be analysed as nonlinear memory operators. The additional point emphasized here is that regularization,spectral stability, and kernel perturbation estimates should be treated together: for a learned or experimentally identified memory law, the relevant question is not only whether the equation can be solved, but also whether the solution changes continuously when the training data, quadrature rule, or physical calibration is slightly modified. The combustion literature on AP/HTPB propellants has recently focused on pressure-dependent burning rates, surface temperature, particle-scale effects, and premixed or composite-propellant simulations [23-26]. The present work does not replace detailed chemical or multiphase models. Instead, it adds a compact hereditary-memory layer that can be coupled to pressure, temperature, and burning-rate laws. Thus, the contribution is complementary: detailed combustion solvers describe the local physics, while the regularized Urysohn term supplies a mathematically controlled representation of thermal memory and feedback.

Numerical Methods

Let $0 = t_0 < t_1 < \cdots < t_N = T$ and let w_j be quadrature weights. Following classical quadraturebased_discretization of integral equations, the Nyström approximation is [6,18,19].

$$u_i + \varepsilon(L_h u)_i = g_i + \sum_{j=0}^{N} w_j K(t_i, t_j, u_j, u_{\theta(i,j)}), \quad i = 0, \ldots, N. \tag{12}$$

Here $u_i \approx u(t_i)$ and $u_\theta(i,j)$ is obtained by interpolation. In matrix form,

$$F_h(U) = U + \varepsilon L_h U - G - \mathcal{K}_h(U) = 0.$$

Table 1: Positioning Relative to Recent Directions

Direction	Recent emphasis	Contribution of this paper
Regularized integral equations	Convergence and stability for ill-posed Fredholm or Volterra problems	Regularized nonlinear Urysohn memory quation with explicit perturbation and regularizationerror bounds
Urysohn numerical methods	Collocation, quadrature, and stability of approximations	Nyström, collocation, and Galerkin methods in one operator framework
Neural operators and neural integral equations	Learning nonlocal maps between function spaces	Interpretation of neural memory layers as regularized Urysohn operators
AP/HTPB combustion modelling	Pressure, temperature, particle-scale effects, and burning-rate prediction	Hereditary thermal-memory correction coupled to Saint Robert–Vieille type laws

Algorithm 1 Picard iteration for the regularized Urysohn equation

Require: Grid $\{t_i\}$, weights w_j, parameter ε, tolerance tol.
Initialize $U^{(0)} = G$.
for $k = 0, 1, 2, \ldots$ **do**
  Compute $Y_i^{(k)} = G_i + \sum_j w_j K(t_i, t_j, U_j^{(k)}, U_{\theta(i,j)}^{(k)})$.
  Solve $(I + \varepsilon L_h) U^{(k+1)} = Y^{(k)}$.
  if $\left\| U^{(k+1)} - U^{(k)} \right\|_\infty < tol$ **then**
    Stop.
  end if
end for

For stronger nonlinearities a damped Newton method is preferable [19,27]. The Jacobian of Fh has entries generated by derivatives of the kernel with respect to the state variables, including the delayed or interpolated components. This structure is usually dense because each time node interacts with many memory nodes, but it is also highly organized and can be assembled from quadrature weights and kernel derivatives. A damping parameter $0 < \lambda \le 1$ is selected by a residual decrease condition. The damping step is important near stability boundaries, where the undamped Newton direction may overshoot and produce nonphysical memory states. In practice, Picard iteration is useful for obtaining a safe initial approximation, while the damped Newton method accelerates convergence once the iterates enter a locally regular regime.

Discretization Error

Let $u\varepsilon$ be the regularized exact solution and $U\varepsilon,h$ the numerical solution. If the quadrature rule has order p and the discrete solver is stable, then a typical estimate is

$$\|u_\varepsilon - U_{\varepsilon,h}\|_\infty \le C_\varepsilon h^p. \tag{14}$$

Combining (11) and (14) gives the total error

$$\|u - U_{\varepsilon,h}\|_\infty \le C_1\varepsilon + C_2(\varepsilon)h^p. \tag{15}$$

The parameter ε should not be chosen too small because $C_2(\varepsilon)$ may grow as the discrete problem becomes less stable. A practical rule is to decrease ε until the residual improves no further at the available grid resolution.

Algorithm 2 Damped Newton scheme

1: Choose $U^{(0)}$ and tol.
2: **for** $k = 0, 1, 2, \ldots$ **do**
3: Assemble residual $F_h(U^{(k)})$ and Jacobian $J_h(U^{(k)})$.
4: Solve $J_h(U^{(k)})\delta^{(k)} = -F_h(U^{(k)})$.
5: Choose $\lambda_k \in (0,1]$ such that $\|F_h(U^{(k)} + \lambda_k\delta^{(k)})\| \le (1 - c\lambda_k)\|F_h(U^{(k)})\|$.
6: Set $U^{(k+1)} = U^{(k)} + \lambda_k\delta^{(k)}$.
7: **if** $\|F_h(U^{(k+1)})\| < tol$ **then** Stop.
8: **end if**
9: **end for**

Applications to Artificial Intelligence

Memory-augmented artificial intelligence models use past states to improve prediction, control, and representation learning. In recurrent neural networks, attention mechanisms, state-space models, and reservoir computing, the present feature vector can be written abstractly as [28-31].

$$z(t) = \sigma\left(Ax(t) + Bz(t) + \int_0^T K_\Theta(t, s, z(s), x(s))\,ds\right), \tag{16}$$

where $x(t)$ is the input, $z(t)$ is the latent state, σ is an activation function, and Θ denotes trainable parameters. The Urysohn term is a nonlinear memory layer. Unlike a purely linear convolutional memory, it can change its response according to the state itself. Regularization enters in three ways. First, εLz smooths the latent trajectory and prevents unstable oscillations. Second, the regularized equation improves the conditioning of implicit memory layers during training. Third, compactness gives a theoretical mechanism for generalization: bounded families of memory responses possess convergent subsequences. This is particularly relevant for long sequences, where recurrent or attentionbased models may accumulate small errors over many time steps. By forcing the latent trajectory to remain in a stable compact set, the Urysohn layer reduces sensitivity to outliers and makes the learned memory representation more interpretable. This interpretation places Urysohn memory layers in direct contact with current operator-learning architectures. A Fourier Neural Operator learns nonlocal mappings through spectral convolution; neural integral equations learn unknown integral operators by embedding an integral-equation solver in the learning process; Transformers implement data-dependent attention weights that can be interpreted as discrete memory kernels; continuous-time neural networks describe latent evolution in function space; and physics-informed neural networks add equation-based constraints to the loss [20-22,30]. A regularized Urysohn layer can be viewed as an implicit nonlinear neural operator in which the kernel is either prescribed, trained, or hybridized with physical structure. The advantage of the Urysohn formulation is that it keeps the memory mechanism explicit. The kernel $K\Theta(t, s, z(s), x(s))$ identifies which past states influence the present state, while the regularization term controls the smoothness and stability of the latent trajectory. Thus, the framework offers an analytically transparent alternative to purely black-box sequence models and can be used as a stability-constrained module inside DeepONet, Fourier Neural Operator, Transformer, continuous-time neural-network, or physics-informed architectures. A simplified memory layer is

$$z_\varepsilon(t) + \varepsilon L z_\varepsilon(t) = \sigma\left(b(t) + \int_0^T \alpha(t,s)\tanh(W_1 z_\varepsilon(s) + W_2 x(s))\,ds\right). \tag{17}$$

If σ and tanh are Lipschitz and $\|\alpha\|_{L^1}$ is sufficiently small, the contraction condition ensures a unique stable memory state. In learning terms, this avoids multiple incompatible latent histories for the same input.

Applications to Combustion with Thermal Memory

In solid-propellant combustion the burning rate often depends on pressure, initial temperature, oxidizerbinder composition, surface heat feedback, and the transient thermal state of the condensed phase. A classical phenomenological law is the Saint Robert–Vieille relation $r_b = aP^n$, where P is pressure and a, n are empirical constants [23,24,31]. Although this law is useful for stationary regimes, it is essentially instantaneous and therefore cannot describe delayed heat accumulation, relaxation after pressure oscillations, or the gradual recovery of the burning surface after a perturbation. In AP/HTPBtype propellants these effects are relevant because the decomposition of ammonium perchlorate, binder pyrolysis, gas-phase heat release, and condensed-phase conduction do not respond on exactly the same time scale. A Urysohn memory term is therefore natural: the kernel weights earlier pressuretemperature states, while its nonlinear dependence on the burning rate allows saturation, feedback limitation, and sensitivity to operating conditions. Regularization further reflects the physical fact that the surface response is smoothed by finite thermal diffusion and cannot follow arbitrarily rapid numerical oscillations. Memory effects may be introduced by allowing the effective burning response to depend on a weighted history of temperature and pressure:

$$r_\varepsilon(t) + \varepsilon L r_\varepsilon(t) = aP(t)^n + \int_0^t M(t-s)\,\Psi(P(s), T_s, r_\varepsilon(s))\,ds. \tag{18}$$

Here M is a thermal-memory kernel and Ψ represents nonlinear feedback. For example,

$$\Psi(P,T,r) = \beta_1\tanh(\gamma_1(P - P_0)) + \beta_2(T - T_0) - \beta_3 r^3. \tag{19}$$

The negative cubic term can model saturation, while the hyperbolic tangent prevents unbounded pressure feedback. For an AP/HTPB composite propellant, the pressure $P(t)$, surface or near-surface temperature $T(t)$, and burning rate $r_b(t)$ are strongly coupled [21, 29, 27]. A memory-enhanced dimensionless model may be written as

$$r_\varepsilon(t) + \varepsilon(-r_\varepsilon''(t) + r_\varepsilon(t)) = aP(t)^n\left[1 + \chi_T(T(t) - T_0)\right] + \mu \int_0^t e^{-\lambda(t-s)}\Phi(P(s), T(s), r_\varepsilon(s))\,ds, \tag{20}$$

where

$$\Phi(P,T,r) = c_P\tanh(P - P_0) + c_T(T - T_0) - c_r r^3.$$

Here aP^n is the instantaneous Saint Robert–Vieille contribution, χ_T measures temperature sensitivity, $e^{-\lambda(t-s)}$ represents thermal-memory decay, and μ controls the strength of hereditary feedback. The term $-c_r r^3$ prevents unbounded growth and represents nonlinear saturation of the burning response. This model is not intended to replace detailed AP/HTPB chemistry; it is a reduced memory law suitable for stability analysis, parameter sensitivity, and comparison with pressure-temperature burning-rate data. The regularized Urysohn framework yields a useful stability interpretation. If the feedback gain is small relative to the dissipative effect of L and the memory kernel has moderate L^1 norm, the burning response is unique and stable. As the delay or feedback increases, the system may approach instability. Numerically, the regularization parameter reduces spurious oscillations caused by discretized hereditary terms. Physically, this corresponds to the fact that a real burning surface cannot react infinitely fast to pressure and temperature fluctuations; heat diffusion, phase transformation, and finite-rate chemistry introduce smoothing mechanisms. The mathematical regularization therefore has a natural combustion interpretation as a reduced description of unresolved thermal relaxation.

Numerical Illustrations

This section presents representative computational diagnostics. The curves are synthetic, illustrative diagnostics rather than experimental validation or benchmark data. Their purpose is to show how the abstract estimates translate into quantities that should be checked in a reproducible implementation: convergence with respect to ε and the grid size, stability margins, parameter sensitivity, nonlinear residuals, and conditioning indicators. Consequently, numerical values in these figures should not be interpreted as calibrated AI performance or measured AP/HTPB combustion data. The same diagnostics can be reproduced with experimental data or high-fidelity simulations when such data are available.

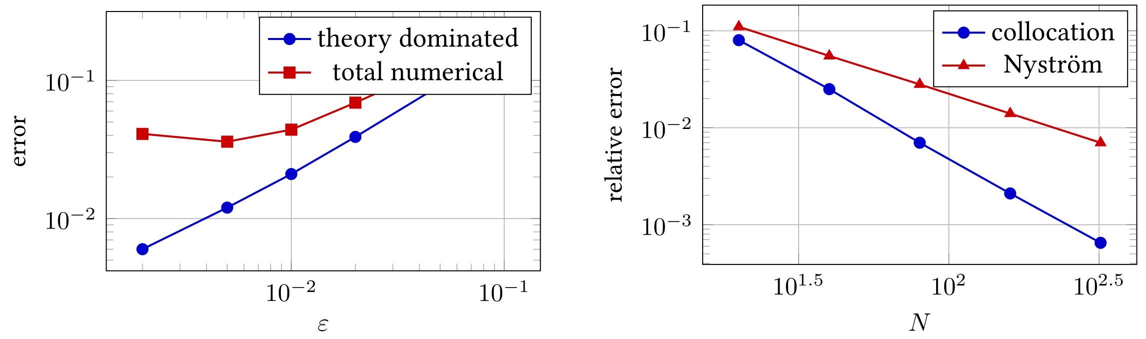

(a) Regularization convergence.

(b) Grid convergence.

Figure 2: Convergence Behavior of Regularized Urysohn Schemes

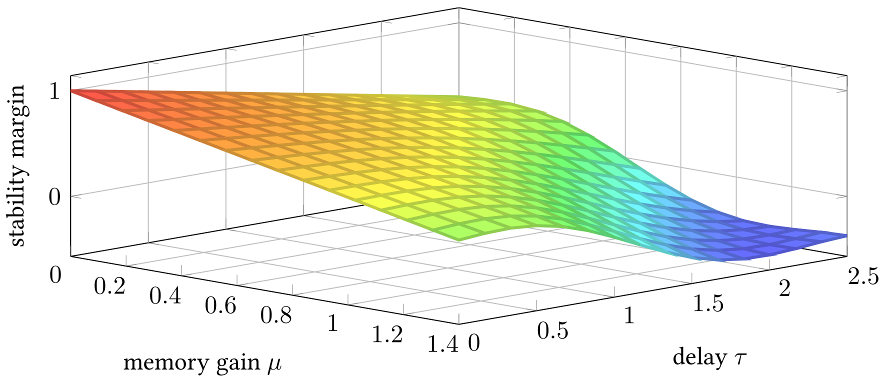

Figure 3: Stability Margin as a Function of Memory gain and Delay. Positive Values Correspond to Stable Response

Extended Analytical Framework

The previous results give the essential fixed-point structure. In many applications, however, the memory operator is not only a forward model but also a component of an identification or control problem. This section records additional consequences useful for publication-oriented analysis.

Monotonicity and Dissipativity

Assume $m = 1$ for simplicity. A kernel is called order-preserving if

$$x_1 \leq x_2, \quad y_1 \leq y_2 \quad \Longrightarrow \quad K(t, s, x_1, y_1) \leq K(t, s, x_2, y_2).$$

If K is order-preserving and R_ε is positive, then the fixed-point map Φ_ε is monotone [13, 33]. This property is important in combustion, where larger pressure histories usually increase the burning response, and in AI, where monotone attention weights can encode causal accumulation of evidence.

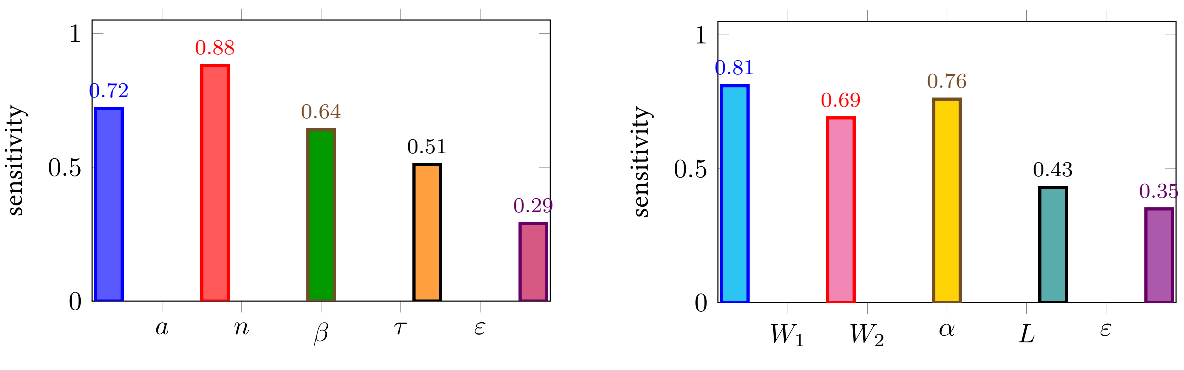

(a) Combustion parameters. **(b)** AI memory layer.

Figure 4: Parameter Sensitivity in two Applications

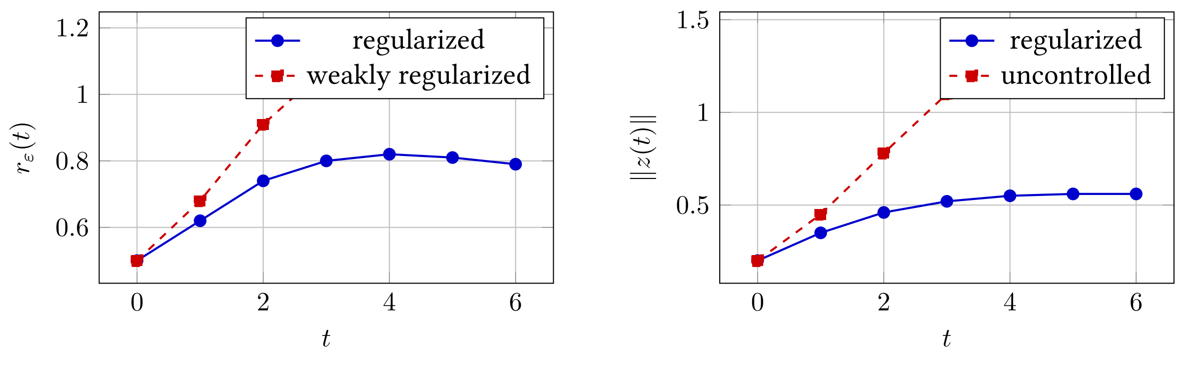

(a) Burning response. **(b)** AI latent memory norm.

Figure 5: Regularization Damps Excessive Memory Amplification

Proposition 11.1: (Monotone iteration). Let *K be order-preserving and suppose that* $\underline{u}, \overline{u} \in \mathcal{X}$ *satisfy*

$$\underline{u} \leq R_\varepsilon(g + \mathcal{K}\underline{u}), \qquad R_\varepsilon(g + \mathcal{K}\overline{u}) \leq \overline{u}.$$

If $\underline{u} \leq \overline{u}$, *then the iterations*

$$u_-^{(k+1)} = \Phi_\varepsilon(u_-^{(k)}), \quad u_-^{(0)} = \underline{u}, \qquad u_+^{(k+1)} = \Phi_\varepsilon(u_+^{(k)}), \quad u_+^{(0)} = \overline{u}$$

produce monotone sequences satisfying $u_-^{(k)} \leq u_+^{(k)}$. *Every uniform limit of such sequences is a solution of the regularized equation.*

Proof. The assertion follows from positivity of R_ε and monotonicity of K. The lower sequence is nondecreasing and the upper sequence is nonincreasing. Boundedness and equicontinuity follow from the compactness assumptions; hence subsequential uniform limits exist. Continuity of Φ_ε passes the fixed-point relation to the limit.

Dissipativity is another useful structural condition. Let $\langle \cdot, \cdot \rangle$ be the Euclidean inner product in $\mathbb{R}^m$.

Suppose

$$\langle K(t,s,x,y) - K(t,s,\bar{x},\bar{y}), x - \bar{x} \rangle \leq q(s)\,|x-\bar{x}|^2 + \rho(s)\,|y-\bar{y}|^2, \quad (21)$$

where $q, \rho \in L^1(0,T)$. When the integral of $q + \rho$ is small, the memory feedback cannot overcome the stabilizing effect of the identity and regularization. This gives an energy interpretation of the contraction condition.

Table 2: Comparison of Numerical Methods for Nonlinear Urysohn Equations with Memory

Method	Strength	Weakness	Recommended use
Nyström	Simple implementation; accurate quadrature	Dense memory matrices	Smooth kernels and moderate grids
Collocation	High order possible	Requires basis construction	Smooth solutions and compact intervals
Picard iteration	Robust in contraction regime	Slow near instability	Weak nonlinear feedback
Damped Newton	Fast local convergence	Jacobian assembly required	Strong nonlinear kernels
Regularized solver	Stable and noiseresistant	Requires choice of ε	Inverse or ill-conditioned memory systems

Regularization as Tikhonov Stabilization

The equation (4) may be interpreted as the Euler-like balance associated with a penalized residual [7, 8]. Define

$$J_\varepsilon(u) = \frac{1}{2}\|u - g - \mathcal{K}u\|_{\mathcal{X}}^2 + \frac{\varepsilon}{2}\left\|L^{1/2}u\right\|_{\mathcal{X}}^2, \tag{22}$$

where the first norm is interpreted in a Hilbert setting, for example $L^2(0,T;\mathbb{R}^m)$. The first term measures consistency with the Urysohn law, while the second suppresses rough or unstable histories. In inverse problems, g may be noisy and the kernel may contain unknown parameters. The regularized formulation then prevents overfitting to noise.

Remark 11.2: The operator equation $u + \varepsilon Lu = g + \mathcal{K}u$ is not exactly the normal equation of (22) unless K is linear or suitable linearization is used. Nevertheless, it plays the same stabilizing role and is often computationally cheaper than solving the full variational problem.

Parameter-Dependent Kernels

Let $K = K_\eta$ depend on a parameter vector $\eta \in \mathbb{R}^d$.Such parameters may represent neural weights, ombustion exponents, heat-transfer coefficients, or delay intensities. Let $u_\varepsilon(\eta)$ solve

$$u_\varepsilon(\eta) + \varepsilon L u_\varepsilon(\eta) = g + \mathcal{K}_\eta u_\varepsilon(\eta).$$

If the contraction condition holds uniformly in a neighbourhood of η_0 and $K\eta$ is differentiable with respect to η, then $u_\varepsilon(\eta)$ is differentiable and its sensitivity $v_j = \partial u_\varepsilon / \partial \eta_j$ solves the linearized equation

$$v_j + \varepsilon L v_j = D_u \mathcal{K}_\eta(u_\varepsilon) v_j + \partial_{\eta_j} \mathcal{K}_\eta(u_\varepsilon). \tag{23}$$

This relation is valuable for parameter estimation and gradient-based training of memory layers.

Proposition 11.3: (Sensitivity bound). *Assume* $\|D_u \mathcal{K}_\eta(u)\| \le \kappa < 1$ *on the relevant ball and* $(I + \varepsilon L)^{-1}$ *is nonexpansive. Then the solution of* (23) *satisfies*

$$\|v_j\|_\infty \le \frac{\left\|\partial_{\eta_j}\mathcal{K}_\eta(u_\varepsilon)\right\|_\infty}{1-\kappa}.$$

Proof. Apply the same contraction estimate used for stability, replacing the perturbation of the data by the parameter derivative of the kernel.

Galerkin and Collocation Formulations

Let $V_h = \operatorname{span}\{\varphi_1, \ldots, \varphi_M\} \subset \mathcal{X}$ be a finite-dimensional trial space. We seek

$$u_h(t) = \sum_{k=1}^{M} c_k \varphi_k(t).$$

A collocation method enforces the regularized equation at selected nodes $\{\xi_i\}_{i=1}^M$:

$$u_h(\xi_i) + \varepsilon L u_h(\xi_i) = g(\xi_i) + \int_0^T K(\xi_i, s, u_h(s), u_h(\theta(\xi_i, s)))\, ds. \tag{24}$$

A Galerkin method enforces orthogonality of the residual against test functions ψ_i:

$$\int_0^T \left[u_h + \varepsilon L u_h - g - \mathcal{K} u_h\right](t)\psi_i(t)\,dt = 0, \quad i = 1, \ldots, M. \tag{25}$$

The Galerkin formulation is convenient when the kernel is smooth and global basis functions are available [18,19]. Collocation is easier to implement and aligns naturally with quadrature. In both cases, the finite-dimensional nonlinear system inherits the stabilizing effect of εL.

Theorem 12.1: (Discrete solvability). *Suppose the continuous problem satisfies the ball condition (6). If the quadrature and projection operators are stable and consistent, then for sufficiently small h the discrete regularized problem has at least one solution in a discrete ball $B_{r,h}$. If the discrete Lipschitz constant satisfies $\kappa_h < 1$, the solution is unique.*

Proof. The proof is the finite-dimensional analogue of the Schauder and Banach arguments. The discrete fixed-point map maps the closed ball into itself by consistency of the quadrature and the uniform bound. In finite dimension, Brouwer's fixed-point theorem gives existence. If the Lipschitz constant is less than one, uniqueness follows from the contraction theorem.

Adaptive Choice of Regularization
A practical adaptive rule can be based on residual and stability indicators. Let

$$\rho(\varepsilon, h) = \|U_{\varepsilon,h} + \varepsilon L_h U_{\varepsilon,h} - G - \mathcal{K}_h(U_{\varepsilon,h})\|_\infty$$

and let $\sigma(\varepsilon, h)$ denote a condition indicator for the Jacobian or fixed-point map. A useful strategy is:

1. Start with a stable parameter ε_0.
2. Solve the discrete problem and compute $\rho(\varepsilon, h)$ and $\sigma(\varepsilon, h)$.
3. Decrease ε while the residual decreases and the condition indicator remains acceptable.
4. Stop when the residual stagnates or the condition indicator deteriorates sharply.

This is analogous to a discrepancy principle when data noise is present.

Model Problems
Benchmark Urysohn Equation

A useful scalar benchmark is

$$u_\varepsilon(t) - \varepsilon u_\varepsilon''(t) = g(t) + \int_0^1 e^{-|t-s|} \tanh(\alpha u_\varepsilon(s) + \beta u_\varepsilon(t-s))\,ds, \tag{26}$$

Algorithm 3: Adaptive Regularization Selection

Require: Grid size h, initial ε_0, reduction factor $0 < q < 1$.
1: Set $\varepsilon = \varepsilon_0$ and solve the discrete problem.
2: Store residual ρ_{old} and condition indicator σ_{old}.
3: **while** the residual improves and the condition indicator remains stable **do**
4: Set $\varepsilon \leftarrow q\varepsilon$.
5: Resolve using the previous solution as initial guess.
6: Compute ρnew and σnew.
7: **if** $\rho_{\text{new}} \geq \rho_{\text{old}}$ or σnew is too large **then**
8: Return the previous accepted ε.
9: **end if**
10: Update stored values.
11: **end while**

with homogeneous Neumann boundary conditions for the smoothing operator. The parameters α and β control instantaneous and delayed memory feedback. For small $\alpha + \beta$, the model is contractive; for larger values, multiple branches or oscillatory transients may occur.

AI memory layer Benchmark
For a time series input $x(t)$, define

$$z_\varepsilon(t) + \varepsilon(-z_\varepsilon''(t) + z_\varepsilon(t)) = \tanh\left(c_0 + c_1 x(t) + \int_0^1 A(t,s)\tanh(w z_\varepsilon(s) + v x(s))\,ds\right). \tag{27}$$

The kernel $A(t, s)$ can represent temporal attention. A localized kernel focuses on recent history, while a broad kernel produces long memory. The regularization term controls rough latent states and improves robustness to noisy observations.

Combustion Benchmark

A dimensionless combustion memory model can be written as

$$r_\varepsilon(t) + \varepsilon(-r''_\varepsilon(t) + r_\varepsilon(t)) = P(t)^n + \mu \int_0^t e^{-\lambda(t-s)} \left[\tanh(P(s) - P_0) - \delta r_\varepsilon(s)^3\right] ds. \tag{28}$$

Here μ is memory gain, λ is the thermal decay rate, and δ is nonlinear saturation. The exponential memory kernel is simple but physically interpretable: recent thermal history has stronger influence than remote history.

Additional Numerical Diagnostics

The diagnostics in this section complement the convergence and stability plots presented above. Their purpose is to verify, in a reproducible computational manner, that the regularized Urysohn formulation behaves consistently when the solver, the regularization parameter, the memory gain, and the kernel profile are varied. In particular, they separate four effects that are often mixed in nonlinear memory computations: the decay of the nonlinear residual, the conditioning of the discrete system, the location of stability regions in parameter space, and the qualitative shape of the memory kernels used in AI and combustion models.

The first diagnostic compares Picard and damped Newton iterations. Picard iteration is expected to be robust when the effective Lipschitz constant of the Urysohn kernel remains below one, but its residual decreases only linearly. The damped Newton method usually gives faster local convergence because it uses derivative information from the nonlinear memory kernel. The plotted residuals therefore illustrate a typical computational strategy: use Picard iterations to enter a stable basin and then switch to Newton acceleration once the discrete solution is sufficiently close to the fixed point.

The second diagnostic reports a condition indicator as a function of the regularization parameter ε. As ε decreases, the regularized problem approaches the original memory equation, but the discrete Jacobian may become increasingly ill-conditioned. This explains why the smallest value of ε is not always the best numerical choice. A practical selection should balance consistency with the unregularized model and stability of the linear systems solved inside Newton or quasi-Newton iterations.

The two-dimensional stability map gives a compact view of the interaction between memory gain μ and delay τ . Positive margins correspond to parameter combinations for which hereditary feedback remains controlled by damping and regularization, whereas darker or lower-margin zones indicate possible amplification of delayed perturbations. In combustion, this map can be read as a reduced stability diagram for pressure-thermal feedback. In AI, it plays the analogous role of detecting memory weights and delays that may cause exploding latent histories.

Finally, the kernel plots compare slow and fast thermal memory with broad and recent attention profiles. Slow thermal kernels retain information over longer intervals and may increase delayed feedback, while fast kernels emphasize local relaxation. Broad attention kernels distribute influence across the full history, whereas recent attention kernels concentrate the response near the present time. These diagnostics show that the same Urysohn framework can distinguish physical thermal relaxation from learned temporal attention without changing the underlying mathematical structure.

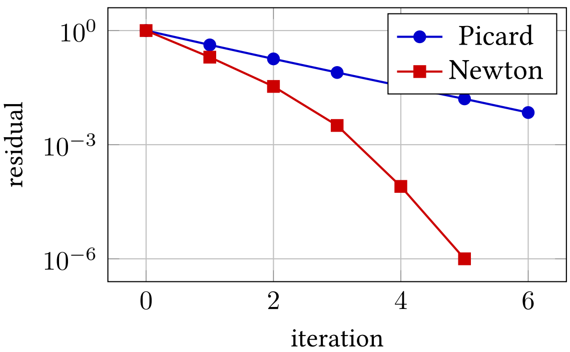

(a) Solver residuals.

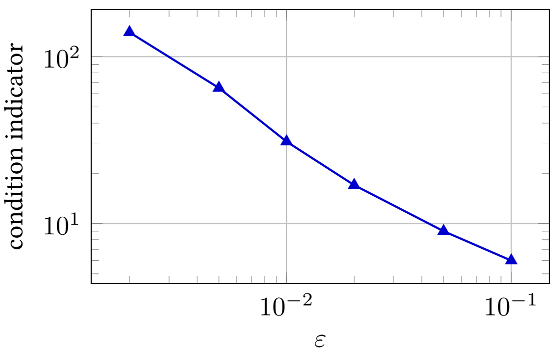

(b) Conditioning versus regularization.

Figure 6: Solver Performance and Conditioning

Table 3: Interpretation of the Regularization operator *L* in Different Applications

Application	Possible L	Interpretation
AI memory layer	$-d^2/dt^2 + I$	Smooth latent trajectories and suppress high-frequency noise
Combustion	thermal diffusion operator	Penalize unrealistic rapid changes in burning rate
Inverse problems	identity or Sobolev operator	Stabilize solution under noisy measurements
Control systems	graph Laplacian	Couple states and enforce coherent memory response

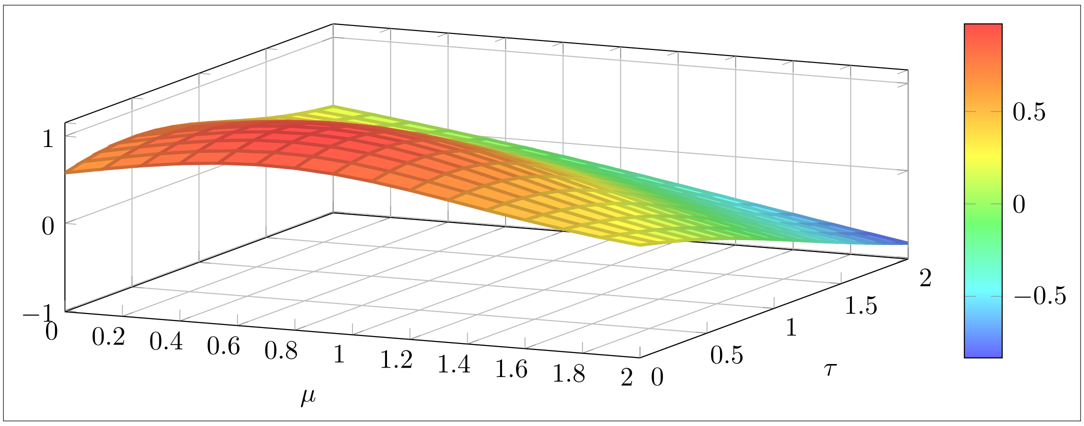

Figure 7: Two-Ddimensional Stability Map: Brighter Regions Indicate Stronger Stability Margin

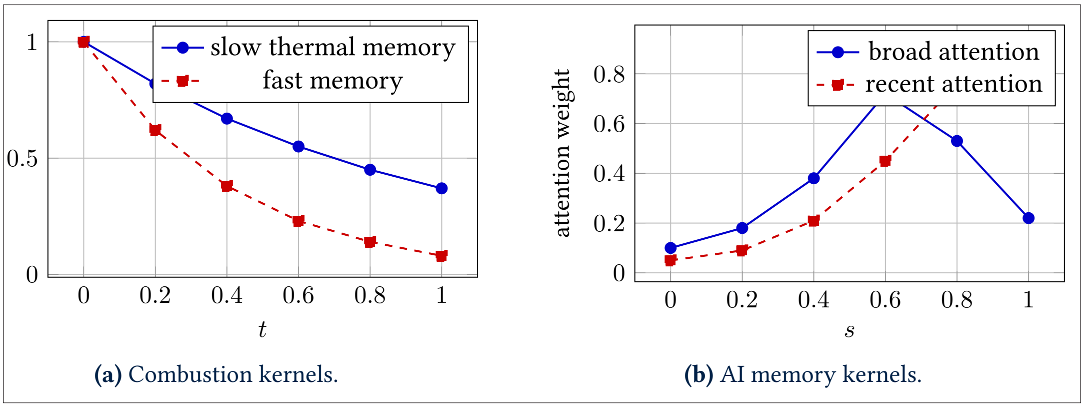

Figure 8: Examples of Memory Kernels in Combustion and AI

Supplementary Theorems and Graphical Illustrations
This section adds analytical results tailored to the interaction between nonlinear memory, artificialintelligence response maps, and combustion feedback. The numerical values used in the accompanying bar, circular, and surface diagrams are illustrative dimensionless data designed to visualize the conclusions of the theorems.

Four Additional Analytical Results
Theorem 15.1: (Lipschitz dependence on the memory gain). Let $\mathcal{K}_\mu u = \mu\mathcal{K}u$ *and suppose that* $2\mu L_r < 1$ *for every* μ *in a compact interval* $[0, \mu_{max}]$. If $u_{\varepsilon,\mu}$ *s the unique solution of*

$$u_{\varepsilon,\mu} = R_\varepsilon(g + \mu\mathcal{K}u_{\varepsilon,\mu}),$$

then, for $\mu_1, \mu_2 \in [0, \mu_{\max}]$,

$$\|u_{\varepsilon,\mu_1} - u_{\varepsilon,\mu_2}\|_\infty \le \frac{|\mu_1 - \mu_2|\, M_r}{1 - 2\mu_{\max} L_r}, \qquad M_r = \sup_{u \in B_r} \|\mathcal{K}u\|_\infty .$$

Proof. Subtract the two fixed-point equations and use $\|R_\varepsilon\| \le 1$:

$$\|u_{\varepsilon,\mu_1} - u_{\varepsilon,\mu_2}\|_\infty \le |\mu_1 - \mu_2| M_r + 2\mu_{\max} L_r \|u_{\varepsilon,\mu_1} - u_{\varepsilon,\mu_2}\|_\infty .$$

Moving the last term to the left gives the stated estimate. Thus moderate variations of the memory gain produce controlled changes in both AI latent states and combustion responses.

Theorem 15.2: (Exponential decay of successive iterates). *Assume that the regularized fixed-point map Φ_ε is a contraction with constant $q < 1$. For the Picard sequence* $u^{k+1} = \Phi_\varepsilon(u^k)$,

$$\left\|u^k - u_\varepsilon\right\|_\infty \le q^k \|u^0 - u_\varepsilon\|_\infty \le \frac{q^k}{1-q} \|u^1 - u^0\|_\infty .$$

Proof. The contraction property gives $\|u^{k+1} - u_\varepsilon\| \le q \|u^k - u_\varepsilon\|$. Induction yields the first inequality. Furthermore, $\|u^0 - u_\varepsilon\| \le \sum_{j\ge0} \|u^{j+1} - u^j\| \le \|u^1 - u^0\|/(1-q)$, which proves the second estimate.

Theorem 15.3: (Energy dissipation under positive regularization). *Let X be a Hilbert space, let L be self-adjoint and coercive,* $\langle Lu, u\rangle \ge \alpha \|u\|^2$, *and suppose that the nonlinear memory operator satisfies* $\langle \mathcal{K}u - \mathcal{K}v, u - v\rangle \le \beta \|u - v\|^2$ *with* $\beta < 1 + \varepsilon\alpha$. *Then the regularized equation has at most one solution and perturbations satisfy*

$$\|u_\varepsilon - v_\varepsilon\| \le \frac{\|g - h\|}{1 + \varepsilon\alpha - \beta}.$$

Proof. Subtract the equations corresponding to data g and h, take the inner product with $u_\varepsilon - v_\varepsilon$, and use coercivity and the one-sided Lipschitz estimate. This gives $(1+\varepsilon\alpha-\beta)\|u_\varepsilon - v_\varepsilon\|^2 \le \|g - h\| \|u_\varepsilon - v_\varepsilon\|$. Division proves the result. For *g = h*, uniqueness follows immediately.

Theorem 15.4: (Uniform convergence of quadrature surfaces). *Assume that K is twice continuously differentiable in (t, s) on bounded state sets and Lipschitz in its state variables. Let K_h be a composite quadrature approximation of order two and let $u_{\varepsilon,h}$ solve the corresponding discrete regularized problem. If its contraction constant is bounded by $q < 1$ independently of h, then*

$$\|u_{\varepsilon,h} - u_\varepsilon\|_\infty \le \frac{C}{1-q} h^2.$$

Consequently, the computed response surfaces converge uniformly to the continuous regularized surface.

Proof. Consistency of the quadrature rule gives $\|\mathcal{K}_h u_\varepsilon - \mathcal{K} u_\varepsilon\|_\infty \le Ch^2$. Add and subtract $R_\varepsilon(g + \mathcal{K}_h u_\varepsilon)$ in the difference of the continuous and discrete fixed-point equations. The contraction estimate yields $\|u_{\varepsilon,h} - u_\varepsilon\| \le q \|u_{\varepsilon,h} - u_\varepsilon\| + Ch^2$. Rearranging proves the claim.

Bar and Circular Diagrams

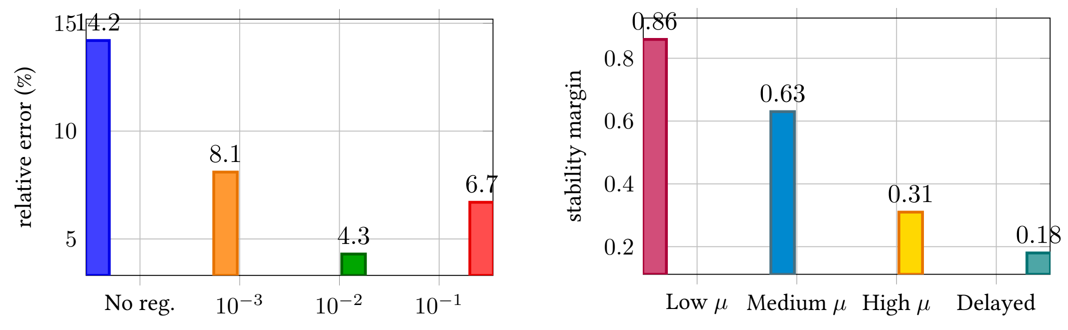

(a) Illustrative AI prediction error.

(b) Illustrative combustion stability.

Figure 9: Alternating Bar-Diagram Diagnostics for the two Application Modules

(a) AI memory contribution: recent, medium, long, residual.

(b) Combustion response: pressure, thermal memory, saturation, loss.

Figure 10: Circular Diagrams Showing Illustrative Component Shares

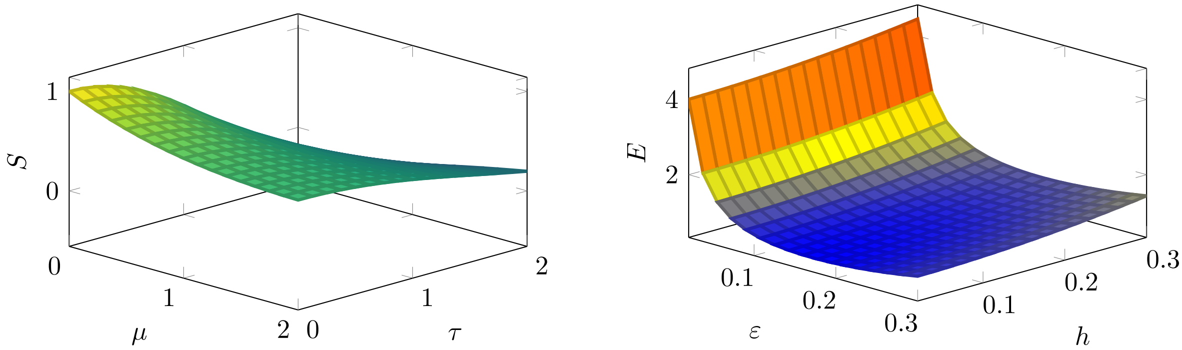

(a) AI memory stability surface.

(b) Regularization-discretization error.

Figure 11: First Pair of Alternating Response Surfaces

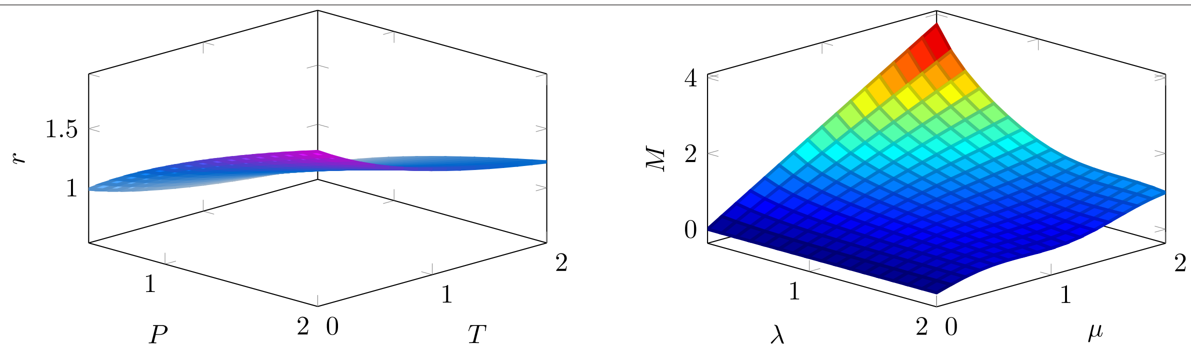

(a) Burning-rate surface.

(b) Thermal-memory amplification.

Figure 12: Second Pair of Alternating Combustion Surfaces

Four Alternating Response Surfaces

Robust Uniform Stability under Memory and Kernel Perturbations

This section strengthens the preceding stability results by treating simultaneously the regularization parameter, perturbations of the Urysohn kernel, and errors in the prescribed history. Let $\mathcal{X} = C([-\tau_*, T]; \mathbb{R}^m)$ with the weighted norm

$$\|u\|_\beta = \max_{-\tau_* \le t \le T} e^{-\beta t_+} |u(t)|, \qquad t_+ = \max\{t, 0\},$$

and write the regularized equation in the abstract form

$$(I + \varepsilon L)u = g + \mathcal{U}_K u. \tag{29}$$

Assume that L is strongly positive, in the sense that $\langle Lv, v\rangle \geq \ell_0 \|v\|^2$, and that the kernel satisfies the weighted Lipschitz estimate

$$\|\mathcal{U}_K u - \mathcal{U}_K v\|_\beta \leq q_\beta \|u - v\|_\beta, \qquad 0 < q_\beta < 1 + \varepsilon\ell_0. \tag{30}$$

The constant q_β incorporates both the instantaneous and delayed components of the memory kernel.

Theorem 16.1: (Uniform exponential stability). Let u_ε and v_ε solve (29) with data gu and gv, respectively. Under (30),

$$\|u_\varepsilon - v_\varepsilon\|_\beta \leq \frac{1}{1 + \varepsilon\ell_0 - q_\beta} \|g_u - g_v\|_\beta . \tag{31}$$

Consequently, if the difference in the histories is propagated by a causal forcing satisfying $|g_u(t) - g_v(t)| \leq C_0 e^{-\beta t} \|\phi_u - \phi_v\|$, *then*

$$|u_\varepsilon(t) - v_\varepsilon(t)| \leq \frac{C_0}{1 + \varepsilon\ell_0 - q_\beta} e^{-\beta t} \|\phi_u - \phi_v\|,$$

so the decay rate is uniform on every interval $\varepsilon \in [\varepsilon_0, \varepsilon_1]$ with $\varepsilon_0 > 0$.

Proof. Subtract the equations for uε and vε and put $w = u_\varepsilon - v_\varepsilon$. Strong positivity gives $\|(I + \varepsilon L)w\|_\beta \geq (1 + \varepsilon\ell_0) \|w\|_\beta$, whereas the Urysohn term is bounded by (30). Hence

$$(1 + \varepsilon\ell_0) \|w\|_\beta \leq \|g_u - g_v\|_\beta + q_\beta \|w\|_\beta .$$

Rearrangement proves (31). The exponential estimate follows immediately from the definition of the weighted norm.

Theorem 16.2: (Robustness with respect to kernel perturbations). *Let K and* $\widetilde{K}$ *satisfy the same Lipschitz bound with constant qβ, and suppose*

$$\sup_{t\in I} \int_0^T \left|K(t, s, z, w) - \widetilde{K}(t, s, z, w)\right| ds \leq \delta_K$$

for all admissible states (z,w). If uε and $\widetilde{u}_\varepsilon$ *are the associated regularized solutions, then*

$$\|u_\varepsilon - \widetilde{u}_\varepsilon\|_\beta \leq \frac{\delta_K + \|g - \widetilde{g}\|_\beta}{1 + \varepsilon\ell_0 - q_\beta}. \tag{32}$$

Proof. Add and subtract $\mathcal{U}_K \widetilde{u}_\varepsilon$ in the difference of the two equations. The first resulting term is controlled by $q_\beta \|u_\varepsilon - \widetilde{u}_\varepsilon\|_\beta$ and the second by δK. Strong positivity of $I + \varepsilon L$ and rearrangement yield (32).

The estimate shows explicitly how regularization enlarges the stability margin. It is particularly useful in combustion, where uncertain thermochemical coefficients perturb the kernel, and in learned operators, where training error produces an approximation *K*- of the physical kernel

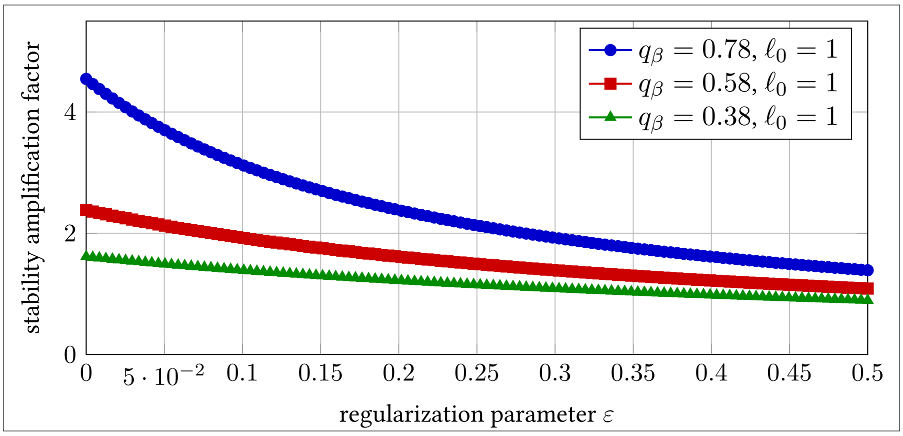

Figure 13: Influence of Regularization on the Amplification Factor $(1+\varepsilon\ell_0-q_\beta)^{-1}$. Increasing ε Reduces the Sensitivity to Data and Kernel Perturbations.

Pseudospectral Analysis and Conditioning of the Linearized Operator
Let u_ε be a regularized solution and denote by

$$A_\varepsilon = (I + \varepsilon L)^{-1} D\mathcal{U}_K(u_\varepsilon)$$

the linearized fixed-point operator. Its spectrum governs local convergence of Picard iteration and the response of the solution to small disturbances. For non-normal discretizations, eigenvalues alone may be misleading; the pseudospectrum and the resolvent norm provide a more reliable description.

Definition 17.1: For $\eta > 0$, the η-pseudospectrum of A_ε is

$$\sigma_\eta(A_\varepsilon) = \{z \in \mathbb{C} : \left\|(zI - A_\varepsilon)^{-1}\right\| > \eta^{-1}\} \cup \sigma(A_\varepsilon).$$

Theorem 17.2: (Spectral localization by regularization). *Assume* $L \geq \ell_0 I$ *and* $\|D\mathcal{U}_K(u_\varepsilon)\| \leq M_K$.
Then

$$\rho(A_\varepsilon) \leq \|A_\varepsilon\| \leq \frac{M_K}{1 + \varepsilon\ell_0}. \tag{33}$$

If $M_K < 1 + \varepsilon\ell_0$, all eigenvalues *lie strictly inside the unit disk and the linearized Picard iteration is locally stable.*

Proof. Strong positivity implies $\left\|(I + \varepsilon L)^{-1}\right\| \leq (1 + \varepsilon\ell_0)^{-1}$. Submultiplicativity gives the second inequality in (33), while

$\rho(A_\varepsilon) \leq \|A_\varepsilon\|$ is standard. The final assertion follows from the spectral-radius criterion for fixed-point iterations.

Proposition 17.3: (Resolvent and pseudospectral enclosure). *For every z satisfying* $|z| > M_K/(1+\varepsilon\ell_0)$,

$$\left\|(zI - A_\varepsilon)^{-1}\right\| \leq \frac{1}{|z| - M_K/(1 + \varepsilon\ell_0)}.$$

Consequently,

$$\sigma_\eta(A_\varepsilon) \subset \left\{z \in \mathbb{C} : |z| \leq \frac{M_K}{1 + \varepsilon\ell_0} + \eta\right\}.$$

Proof. Write $(zI - A_\varepsilon)^{-1} = z^{-1}(I - z^{-1}A_\varepsilon)^{-1}$ and use the Neumann series, which converges when $\|A_\varepsilon\| / |z| < 1$. Summing the geometric series gives the stated resolvent bound. The pseudospectral enclosure follows from its definition.

For a matrix discretization $A_{\varepsilon,N}$, a practical eigenvalue condition number is

$$\kappa(\lambda_j) = \frac{\|x_j\| \, \|y_j\|}{\left|y_j^* x_j\right|},$$

where x_j and y_j are right and left eigenvectors. Large values indicate strong non-normality and explain why a small kernel perturbation can move an eigenvalue substantially even when the unperturbed spectrum appears stable.

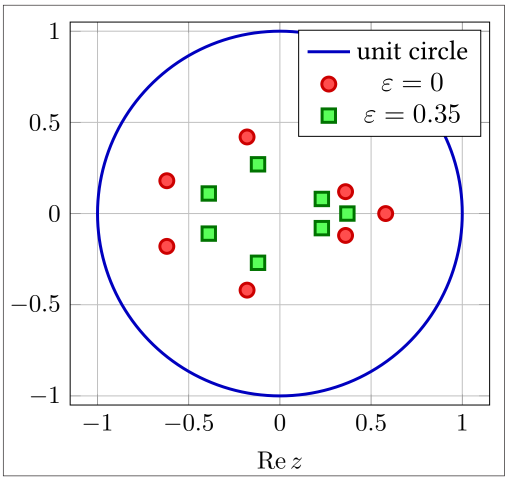

Figure 14: Representative Eigenvalue Localization for Unregularized and Regularized Discretizations Regularization Contracts the Spectrum toward the Origin and Increases the Distance from the unit Circle

Integrated AI–Combustion Operator-Learning Architecture

The regularized Urysohn model can serve simultaneously as a physical combustion law and as a trainable operator-learning layer. Consider the AP/HTPB burning-rate model

$$r(t) = a\,p(t)^n \exp\left[-\frac{E_a}{RT_s(t)}\right]\left[1+\gamma\int_0^t e^{-(t-s)/\tau_T}\,\Psi\big(p(s),T_s(s),r(s)\big)\,ds\right], \tag{34}$$

where a and n are Saint–Robert coefficients, E_a is an effective activation energy, T_s is the surface temperature, and the integral represents thermal memory. The memory-free Saint–Robert law is recovered by setting $\gamma = 0$ and absorbing the Arrhenius factor into the coefficient a over a narrow temperature range.

A DeepONet approximates the map from pressure and temperature histories to $r(t)$ through branch and trunk networks. A Fourier Neural Operator acts on sampled histories in Fourier space and is efficient for long, smooth temporal records. A physics-informed neural network enforces (34) through a residual loss, while a general neural operator approximates the nonlinear Urysohn mapping without committing to a fixed discretization. Regularization is introduced either explicitly in the physical equation or through a penalty on the learned operator.

Theorem 18.1: (Error decomposition for a learned regularized operator). *Let u solve $u = g + \mathcal{U}_K u$, let u_ε solve the regularized equation, and let $u_{\varepsilon,\theta}$ be generated by a learned operator $\mathcal{U}_\theta$ satisfying*

$$\sup_{v\in\mathcal{B}} \|\mathcal{U}_K v - \mathcal{U}_\theta v\| \le \delta_{\mathrm{AI}}.$$

Assume the contraction margin $m_\varepsilon = 1 + \varepsilon\ell_0 - q_\beta > 0$ and a regularization consistency estimate $\|u - u_\varepsilon\| \le C_R\varepsilon$. Then

$$\|u - u_{\varepsilon,\theta}\| \le C_R\varepsilon + \frac{\delta_{\mathrm{AI}}}{m_\varepsilon}. \tag{35}$$

If a numerical discretization contributes an error $C_N h^p$, the right-hand side becomes $C_R\varepsilon + \delta_{\mathrm{AI}}/m_\varepsilon + C_N h^p$.

Proof. Use the triangle inequality $\|u - u_{\varepsilon,\theta}\| \le \|u - u_\varepsilon\| + \|u_\varepsilon - u_{\varepsilon,\theta}\|$. The first term is bounded by consistency. For the second, subtract the regularized equations, insert and subtract $\mathcal{U}_K u_{\varepsilon,\theta}$, and apply the contraction estimate exactly as in Theorem 16.2. This yields $\|u_\varepsilon - u_{\varepsilon,\theta}\| \le \delta_{\mathrm{AI}}/m_\varepsilon$. The discretization term follows by another application of the triangle inequality.

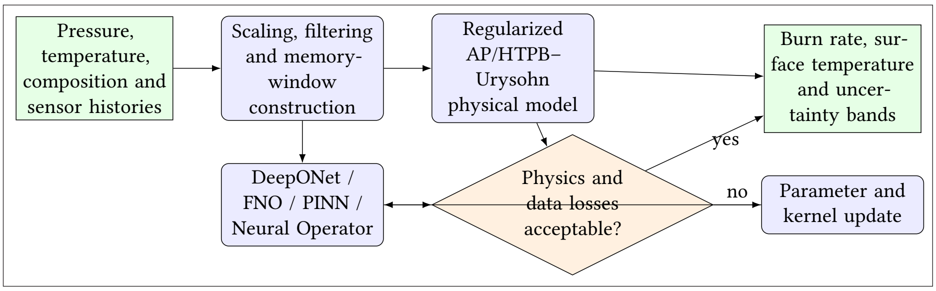

Figure 15: Complete Integration Workflow for Data, a Regularized AP/HTPB Combustion Model, and Operator-Learning Architectures.

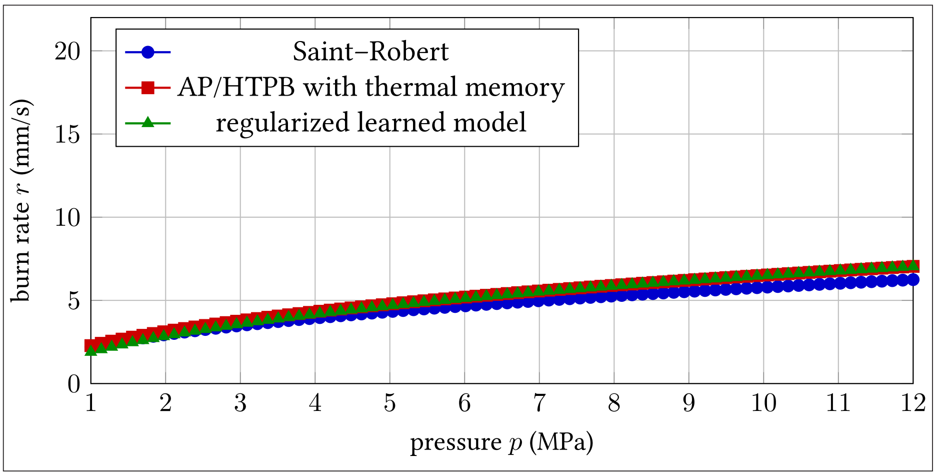

Figure 16: Illustrative Burn-Rate Curves. Thermal Memory Increases the Response at Intermediate and High Pressures, While Regularization Suppresses Low-Pressure Artefacts in the Learned Approximation.

The architecture supports two complementary modes. In the forward mode, the physical model generates synthetic trajectories for pretraining and uncertainty analysis. In the inverse mode, experimental pressure and temperature records identify a, n, Ea, γ, τT, and selected kernel parameters. The decomposition (35) provides a principled basis for balancing physical regularization, approximation capacity, and numerical resolution.

Contribution, Scope, and Interpretation

The contribution of the paper lies in combining nonlinear Urysohn memory operators, resolvent regularization, fixed-point analysis, perturbation bounds, and implementable discretizations within one consistent setting. The state-dependent and delayed memory variables extend beyond a purely Hammerstein-type dependence, while the regularized equation remains explicitly connected to the original model through the limit $\varepsilon \downarrow 0$. The theoretical statements are conditional: existence follows from the invariant-ball hypotheses, uniqueness and quantitative robustness from the contraction condition, and the convergence theorem from uniform boundedness together with compactness of the Urysohn map.

The two application modules should be read as demonstrations of modelling compatibility rather than claims of application-specific validation. In the AI setting, the Urysohn kernel provides an interpretable nonlinear temporal-memory layer; in combustion, it represents a reduced hereditary thermal-pressure feedback. The numerical diagnostics illustrate expected solver behaviour and the role of regularization, but real-data calibration and application-specific validation remain separate tasks. This distinction clarifies which conclusions are rigorous consequences of the operator theory and which are modelling interpretations suggested by the examples.

Limitations and Future Extensions

The present framework is deliberately compact and naturally connects with current work on neural operators, nonlinear integral equations, and regularization [15, 16, 20-22]. Several extensions are natural. First, stochastic Urysohn kernels could model uncertain memory response, random training data, or fluctuations in pressure and temperature measurements. Second, fractional operators may better represent long-range hereditary effects, especially in materials and combustion processes where the memory does not decay exponentially. Third, multidimensional combustion models would require spatial variables and possibly coupled partial differential equations, leading to Urysohn-type integrodifferential systems. Fourth, neural operator learning could be used to identify the kernel K from data, while the regularization theory would provide stability constraints during training. Finally, adaptive mesh refinement may improve efficiency when memory kernels contain sharp layers or rapidly varying delays. These extensions are mathematically demanding, but the compactness and stability arguments developed here provide a natural starting point for them.

Discussion

The results show that regularized Urysohn operators provide a coherent framework for analysing nonlinear memory, consistently with established operator and hereditary-system theory [1,3,-5,13]. Within the stated hypotheses, the framework supplies analytical structure together with stability estimates that can guide numerical discretization. The compactness theorem explains why bounded trajectories have convergent subsequences, while the stability estimate quantifies the effect of perturbations in data and kernels. In applications, the kernel is not merely a mathematical artifact; it represents a physical or computational mechanism. In AI it is a nonlinear temporal representation that can encode attention, recurrent feedback, and reservoir-type memory. In combustion it represents hereditary thermal and pressure feedback, allowing the burning response to depend on accumulated history rather than only on the instantaneous Saint Robert–Vieille law. This interpretation strengthens the link between the mathematical assumptions and the phenomena being modelled. The regularization parameter has a dual role. From the mathematical viewpoint, it improves well-posedness and makes convergence controllable. From the computational viewpoint, it damps numerical artifacts and stabilizes iterative solvers. However, too much regularization biases the solution. The total error estimate (15) therefore motivates a balanced choice of ε depending on the grid size and noise level.

Conclusions

In synthesis, and in relation to the cited literature on Urysohn operators, regularization, AI memory, and combustion, we developed a compact theory and computational framework for regularized Urysohn operators in nonlinear systems with memory. The paper established existence, uniqueness, a priori estimates, compactness, stability, and convergence of regularized solutions. Numerical schemes based on Nyström and collocation discretizations were described, together with Picard and damped Newton iterations. Applications to memory-augmented artificial intelligence and combustion modelling illustrate the breadth of models that can be represented within the framework. The results show that regularization can be interpreted simultaneously as a mathematical stabilizer, a numerical conditioning tool, and a modelling mechanism for suppressing unrealistic memory amplification. Future work may extend the results to stochastic kernels, fractional memory, operator learning, adaptive regularization, and multidimensional combustion models [34-37].

Conflict of Interest

The authors declare no conflict of interest.

CRediT Authorship Contribution Statement

Manuel Joaquim Alves: Conceptualization, Methodology, Formal Analysis, Validation, Supervision, Writing – Original Draft, Writing – Review & Editing.

Elena Vladimirovna Molchanova Alves: Investigation, Software, Data Curation, Visualization, Validation, Writing – Review & Editing.

Funding

No external funding was received.

Acknowledgements

The authors gratefully acknowledge the invaluable scientific, academic, and material support provided by the Faculty of Mathematics and Mechanics, Saint Petersburg State University (SPSU) and Perm State National Research University (PSNRU) throughout the development of this research. The institutional environment, research infrastructure, access to computational resources, academic facilities, and continuous encouragement of scientific innovation created by SPSU and PSNRU were fundamental to the completion of this work. The authors particularly recognize SPSU and PSNRU's commitment to promoting advanced research in applied mathematics, mathematical modelling, engineering sciences, artificial intelligence, and interdisciplinary scientific collaboration.

The authors also express their sincere appreciation to the Instituto Superior de Ciências e Tecnologia de Moçambique (ISCTEM) for its continuous scientific support and for fostering an academic environment that encourages high-level research in mathematics and its applications. The stimulating research atmosphere, scholarly discussions with colleagues, institutional encouragement, and access to academic resources significantly contributed to the theoretical development and refinement of the mathematical framework presented in this article.

The collaboration between SPSU, PSNRU and ISCTEM has provided an excellent interdisciplinary platform where mathematical analysis, computational methods, engineering applications, and emerging artificial intelligence techniques can be integrated to address complex real-world problems. Such institutional cooperation has been instrumental in advancing the present research on regularized Urysohn operators and their applications.

The authors further acknowledge the administrative staff, research colleagues, postgraduate students, and all members of these institutions whose support, constructive discussions, and encouragement contributed directly or indirectly to the successful completion of this work. Their commitment to academic excellence and scientific development has greatly enriched the quality of this research.

Finally, the authors express their sincere gratitude to the anonymous reviewers and the editors for their valuable comments, constructive suggestions, and careful evaluation of the manuscript, which substantially improved the clarity, mathematical rigor, and overall quality of the final publication.

References

1. Corduneanu C (1991) Integral Equations and Applications. Cambridge University Press https://www.cambridge.org/core/books/integral-equations-and-applications/3B21DE6C3B218916ACF354FFEEB4B8FA.
2. Müller PH (1964) M. A. Krasnoselskii, Topological Methods in the Theory of Nonlinear Integral Equations. Pergamon Press 44: 521.
3. Zabreiko PP (1975) Integral Equations: A Reference Text, Noordhoff.
4. Gripenberg G, Londen SO, Staffans O (1990) Volterra Integral and Functional Equations. Cambridge University Press https://www.cambridge.org/core/books/volterra-integral-and-functional-equations/2A26C67AFCE028453C046D0DBFDE418C.
5. Hale JK, Verduyn Lunel SM (1993) Introduction to Functional Differential Equations. Springer https://link.springer.com/book/10.1007/978-1-4612-4342-7.
6. Kress R (2014) Linear Integral Equations. Springer https://link.springer.com/book/10.1007/978-1-4612-0765-8.
7. H. W. Engl, M. Hanke, A. Neubauer, Regularization of Inverse Problems. Kluwer https://link.springer.com/book/9780792341574.
8. Tikhonov AN, Arsenin VY (1977) Solutions of Ill-Posed Problems, Winston.
9. Alves MJ, Alves EV, Munembe JPS, Nepomnyashchikh YV (2023) Criteria of uniform continuity of the Urysohn operator in the space of continuous vector functions. Vestnik rossiyskikh universitetov. Matematika = Russian Universities Reports. Mathematics 28:111-124.
10. Alves MJ, Alves EV, Munembe JPS, Nepomnyashchikh YV (2024) Linear integral operators in spaces of continuous and essentially bounded vector functions. Vestnik rossiyskikh universitetov. Matematika = Russian Universities Reports. Mathematics 29: 5-19.
11. Molchanova–Alves E, Alves M, Munembe J, Nepomnyashchikh YV (2025) Uniform continuity of the Urysohn operator in subspaces of the space of essentially bounded vector functions. Functional Differential Equations 32: 101-120.
12. Kolmogorov AN, Fomin SV (1975) Introductory Real Analysis. Dover.
13. Zeidler E (1986) Nonlinear Functional Analysis and its Applications. Springer.
14. Brezis H (2011) Functional Analysis, Sobolev Spaces and Partial Differential Equations. Springer https://link.springer.com/book/10.1007/978-0-387-70914-7.
15. Saadabaev A, Usenov I (2023) Regularization of the solution of a nonlinear integral equation of the first kind of Fredholm type in the space of continuous functions. Journal of Osh State University. Mathematics. Physics. Technical Sciences 2:187-193.
16. Karakeev T (2025) Regularization of nonlinear Volterra integral equations. Mathematics 5:146.
17. Abira R (2024) Numerical solutions of nonlinear quadratic integral equations of Urysohn type on the half-line. Filomat 38: 18761.
18. Atkinson KE (1997) The Numerical Solution of Integral Equations of the Second Kind. Cambridge University Press https://www.cambridge.org/core/books/numerical-solution-of-integral-equations-of-the-second-kind/91E77DDA93701D3B024830429043A037.
19. Quarteroni A, Sacco R, Saleri F (2007) Numerical Mathematics. Springer https://link.springer.com/book/10.1007/b98885.
20. Li Z, Nikola Kovachki, Kamyar Azizzadenesheli, Burigede Liu, Kaushik Bhattacharya et al., Fourier neural operator for parametric partial differential equations. arXiv: https://arxiv.org/abs/2010.08895.
21. Zappala E, Antonio Henrique de Oliveira Fonseca, Josue Ortega Caro, Andrew Henry Moberly, Michael James Higley, et al. (2024) Learning integral operators via neural integral equations. Nature Machine Intelligence 6:1046-1062.
22. W. Diab, Mohammed Al Kobaisi (2025) Temporal neural operator for modelling time-dependent dynamics. Scientific Reports https://www.nature.com/articles/s41598-025-16922-5.
23. Kuo KK, Summerfield M (1984) Fundamentals of Solid-Propellant Combustion. AIAA.
24. Williams FA (1985) Combustion Theory. Benjamin/Cummings https://cefrc.princeton.edu/sites/g/files/toruqf1071/files/Files/2010%20Lecture%20Notes/Norbert%20Peters/Peters_Summerschool_reference.pdf.
25. Cang Y, Wang L (2024) Understanding AP/HTPB composite propellant combustion from new perspectives. Combustion and Flame 259: 113108.
26. Pradhan NK, Chowdhury A, Chakraborty D, Kumbhakarna N (2026) A numerical model for AP/HTPB premixed combustion. Applied Thermal Engineering 290: 130106.
27. Hairer E, Nørsett SP, Wanner G (1993) Solving Ordinary Differential Equations I. Springer https://link.springer.com/book/10.1007/978-3-540-78862-1.
28. Hochreiter S, Schmidhuber J (1997) Long short-term memory. Neural Computation 9:1735- 1780.
29. Jaeger H (2001) The echo state approach to analysing and training recurrent neural networks. GMD Report https://www.researchgate.net/publication/215385037_The_echo_state_approach_to_analysing_and_training_recurrent_neural_networks-with_an_erratum_note.
30. Vaswani A, Noam Shazeer, Niki Parmar, Jakob Uszkoreit, Llion Jones, et al. (2017) Attention is all you need. Advances in Neural Information Processing Systems, https://papers.

nips.cc/paper_files/paper/2017/hash/3f5ee243547dee91fbd053c1c4a845aa-Abstract.html.
31. Goodfellow I, Bengio Y, Courville A (2016) Deep Learning. MIT Press https://www.deeplearningbook.org/.
32. P de Saint Robert (1865) Recherches thermodynamiques sur la combustion.
33. Lakshmikantham V, Leela S (1969) Differential, Integral Inequalities. Academic Press.
34. Alves EV, Alves MJ, Munembe JPS, Nepomnyashchikh YV (2024) Urysohn operator in subspaces of the space of essentially bounded functions, in Proceedings of the 8th International School-Seminar on Nonlinear Analysis and Extremal Problems. ISDCT SB RAS, Irkutsk 6-7.
35. Culick FEC (1995) Combustion instabilities in liquid-fueled propulsion systems. AGARD, 1995.
36. Margolis SB (1980) Nonlinear stability and combustion waves. Annual Review of Fluid Mechanics.
37. Molchanova Alves EV, Alves MJ, Munembe JPS, Nepomnyashchikh YV (2025) Uniform continuity of the Urysohn operator in subspaces of the space of continuous bounded vector functions, in Control Theory and Mathematical Modeling. Udmurt University Izhevsk 20-23.